Electronic Supplementary Information

Bipyridine hydrogel for selective and visible detection and absorption of Cd^{2+}

Qingqing Miao,[a] Ziye Wu,[c] Zijuan Hai,[a] Changlu Tao,[d] Qingpan Yuan,[a] Yadi Gong,[a] Yafeng Guan,[b] Jun Jiang,[c] and Gaolin Liang*[a]*

[a]CAS Key Laboratory of Soft Matter Chemistry, Department of Chemistry, University of Science and Technology of China, Hefei, Anhui 230026, China

[b]Key Laboratory of Separation Sciences for Analytical Chemistry, Dalian Institute of Chemical Physics, Chinese Academy of Sciences, Dalian 116023, China

[c]Department of Chemical Physics, University of Science and Technology of China, 96 Jinzhai Road, Hefei, Anhui 230026, China.

[d]Center for Integrative Imaging, Hefei National Laboratory for Physical Sciences at the Microscale & School of Life Sciences, University of Science and Technology of China, Hefei, Anhui 230026, China

E-mail: jiangj1@ustc.edu.cn (J.J.), gliang@ustc.edu.cn (G.-L. L.).

Contents:

1. Synthetic route for 1.

2. Supporting Figures.

3. Supporting Tables.

4. References.

1. Synthetic route for 1.

*Preparation of **1**.*

Scheme S1. Synthetic route for compound **1**.

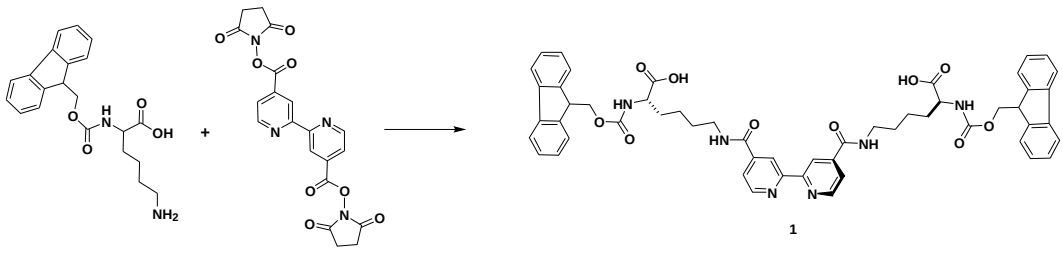

Synthesis of 4,4'-Dicarboxysuccinimidyl-2,2'-bipyridine:

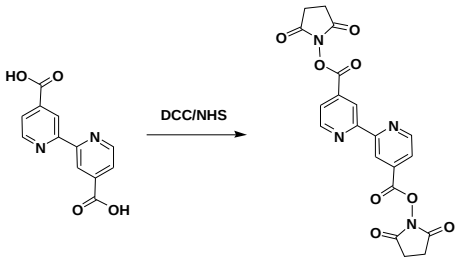

2. Supporting Figures.

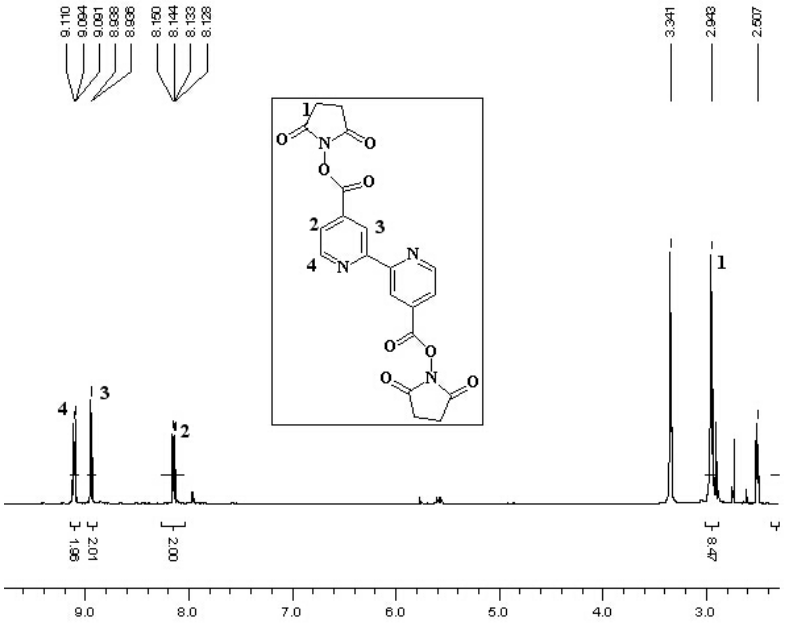

Figure S1. ^{1}H NMR spectrum of compound 4,4'-dicarboxysuccinimidyl-2,2'-bipyridine.

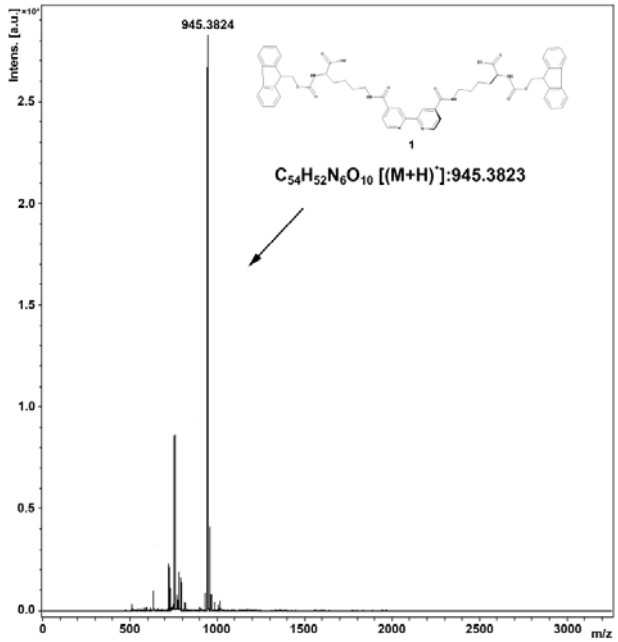

Figure S2. HR-MALDI-TOF/MS spectrum of **1**.

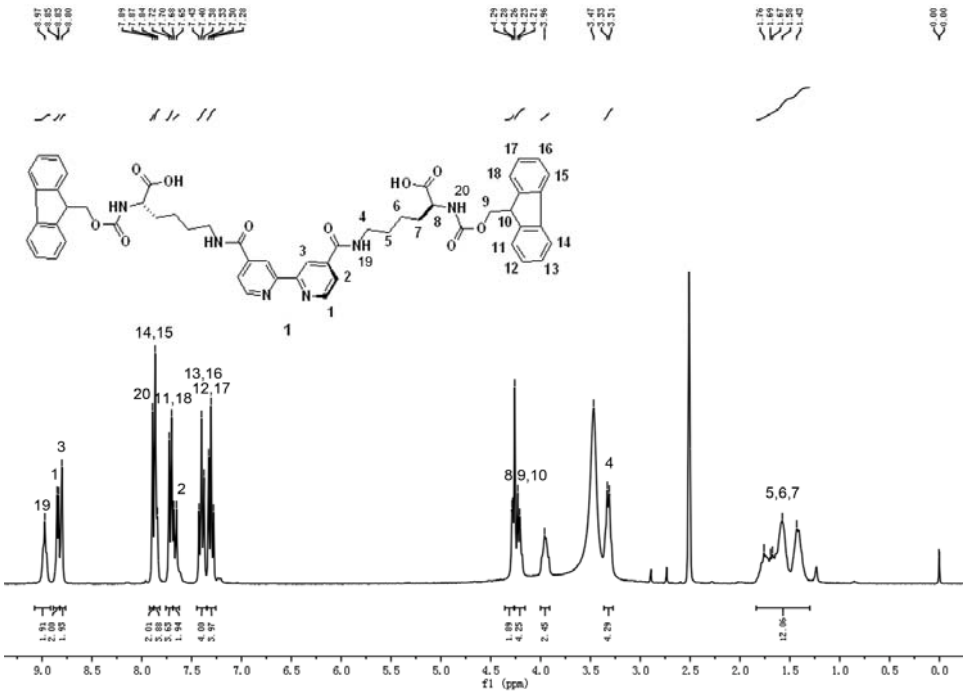

Figure S3. ^{1}H NMR spectrum of compound **1**.

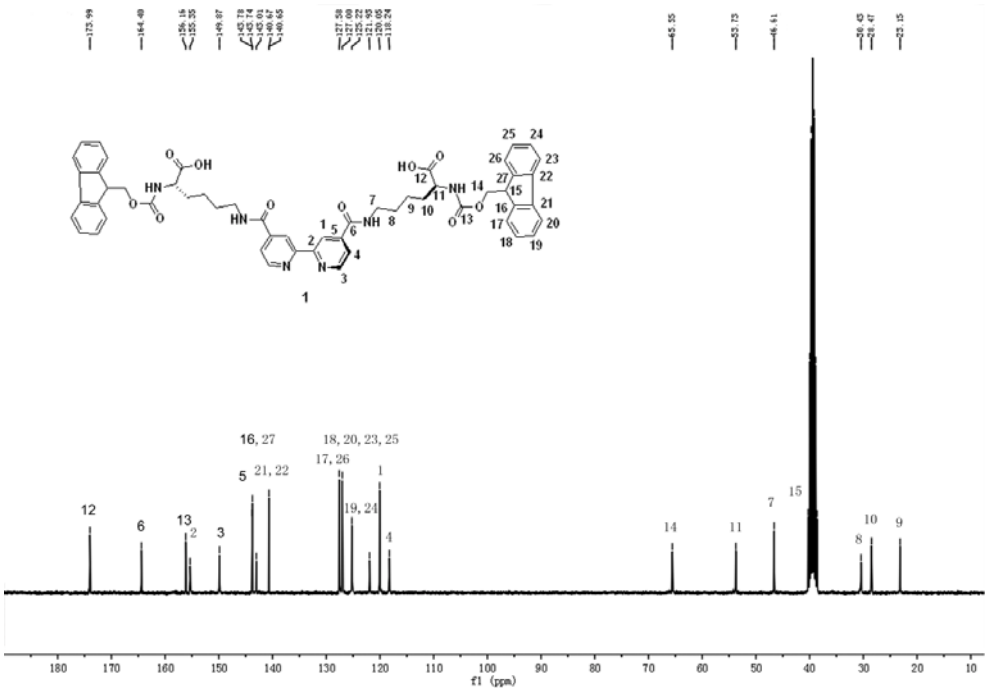

Figure S4. ^{13}C NMR spectrum of compound **1**.

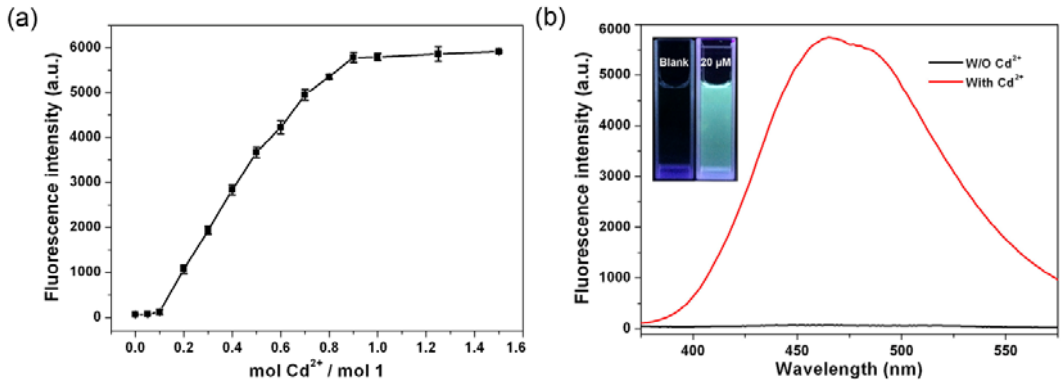

Figure S5. (a) Correlation of fluorescence intensities at 470 nm of **1** (20 μM, λ_{ex} = 300 nm) in the presence of various concentrations of Cd^{2+} (0, 1, 2, 4, 6, 8, 10, 12, 14, 16, 18, 20, 25 or 30 μM) in phosphate buffer (10 mM, pH 7.5) containing 10% ethanol at RT. (b) Fluorescence spectra of **1** (20 μM, λ_{ex} = 300 nm) in the presence of 0, or 20 μM Cd^{2+} in phosphate buffer (10 mM, pH 7.5) containing 10% ethanol at RT. The inset fluorescent photographs show the fluorescence changes of **1** at 20 μM before and after addition of 20 μM Cd^{2+} under a UV lamp.

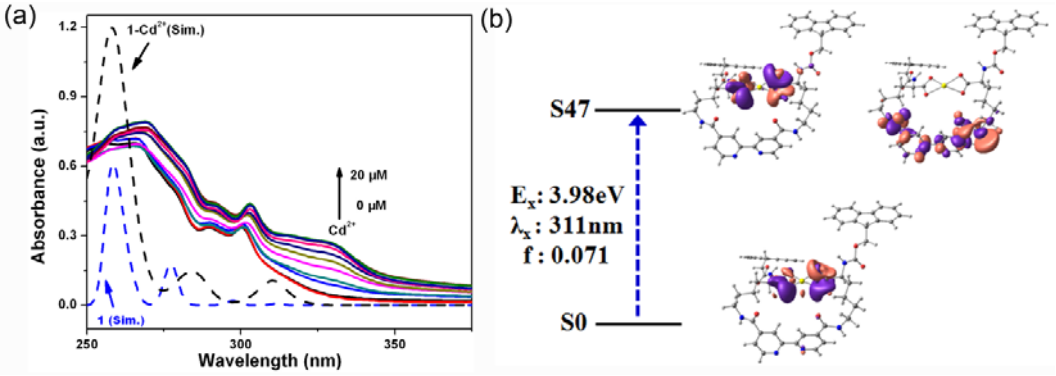

Figure S6. (a) UV-vis absorption spectra of **1** (20 μM) in the presence of various concentrations of Cd^{2+} in phosphate buffer (10 mM, pH 7.5) containing 10% ethanol at RT. The simulated (Sim.) spectra of **1** and **1**-Cd^{2+} are given with dashed curves. (b) The transition energy and orbitals responsible for the absorption peak at around 311 nm of **1**-Cd^{2+}.

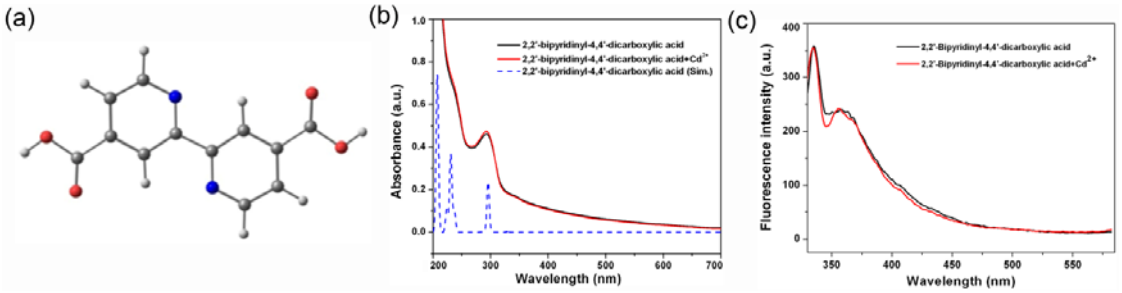

Figure S7. (a) Theoretically optimized molecular structure of 2,2'-bipyridinyl-4,4'-dicarboxylic. (b) UV-vis absorption spectra of 2,2'-bipyridinyl-4,4'-dicarboxylic acid (20 μM) in the presence of Cd^{2+} at 0, or 20 μM in phosphate buffer (10 mM, pH 7.5) containing 10% ethanol at RT. The simulated spectrum is given as blue dashed line. (c) The corresponding fluorescence spectra of 2,2'-bipyridinyl-4,4'-dicarboxylic acid (20 μM) in the presence of Cd^{2+} at 0, or 20 μM, excited at 300 nm.

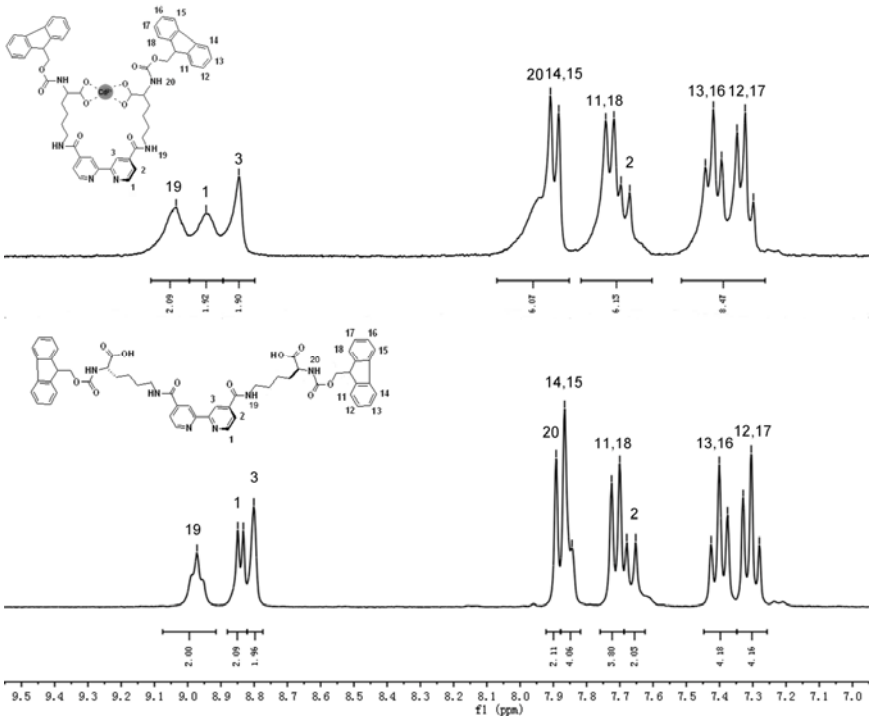

Figure S8. ^{1}H NMR spectra (300 MHz) of **1** (bottom) and **1** upon addition of Cd^{2+} (top) in d_6-DMSO.

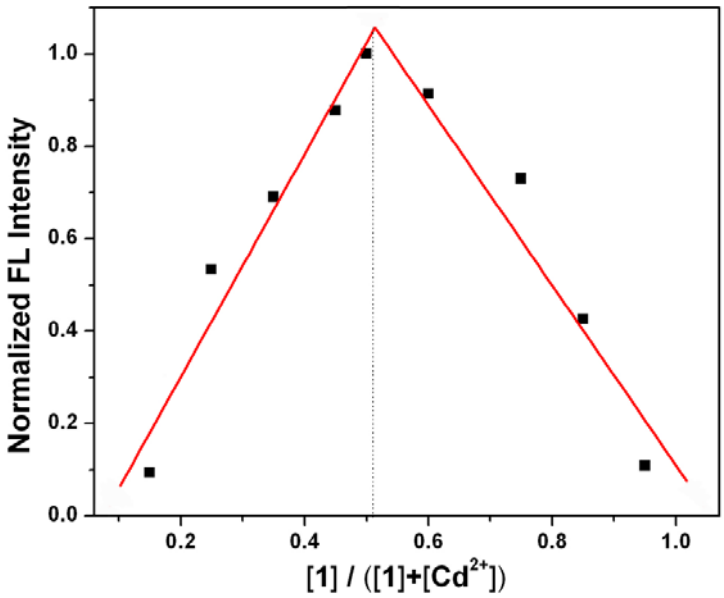

Figure S9. Job' plots of fluorescence intensity changes at varying mole ratios of **1** with Cd^{2+} ([**1**] + [Cd^{2+}] = 40 μM).

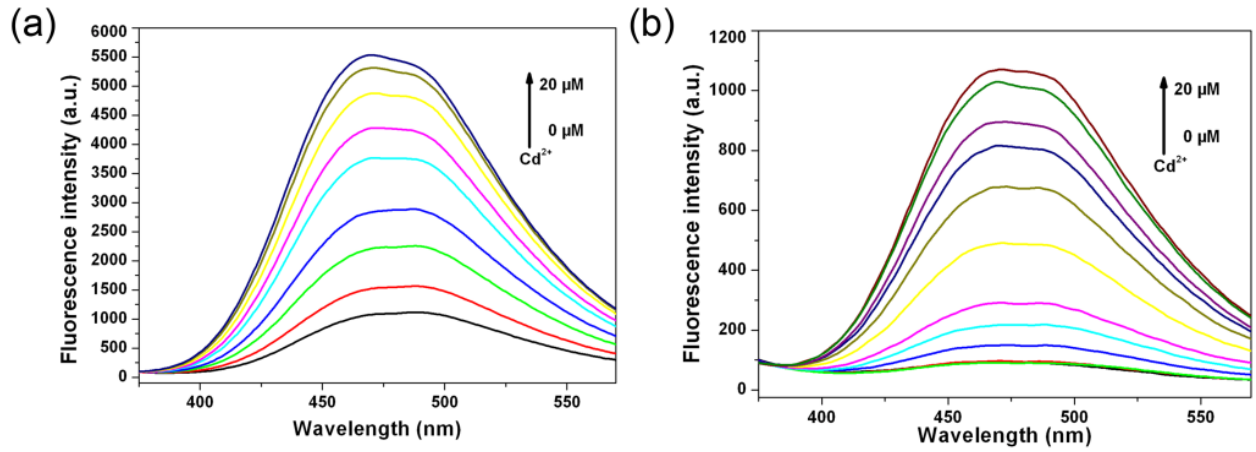

Figure S10. (a) Fluorescence spectra of **1** (20 μM, λ_{ex} = 300 nm) in the presence of various concentrations of Cd^{2+} in phosphate buffer (10 mM, pH 6) containing 10% ethanol at room temperature. (b) Fluorescence spectra of **1** (20 μM, λ_{ex} = 300 nm) in the presence of various concentrations of Cd^{2+} in phosphate buffer (10 mM, pH 9) containing 10% ethanol at room temperature.

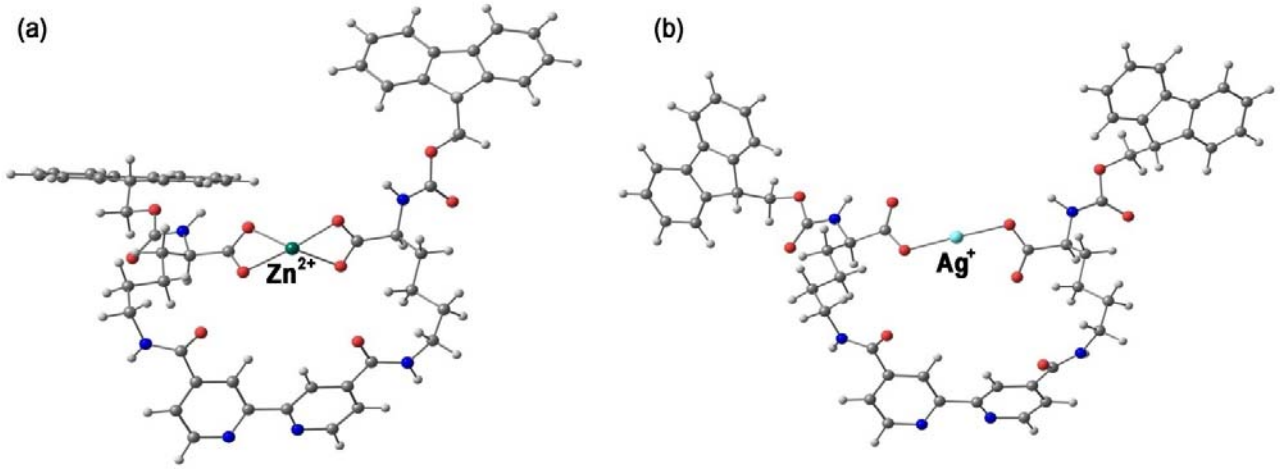

Figure S11. (a) Zn^{2+} forms effective bondings with four oxygen atoms in the **1**-Zn^{2+} complex. (b) Ag^{+} forms weakly bondings with two oxygen atoms in the **1**-Ag^{+} complex.

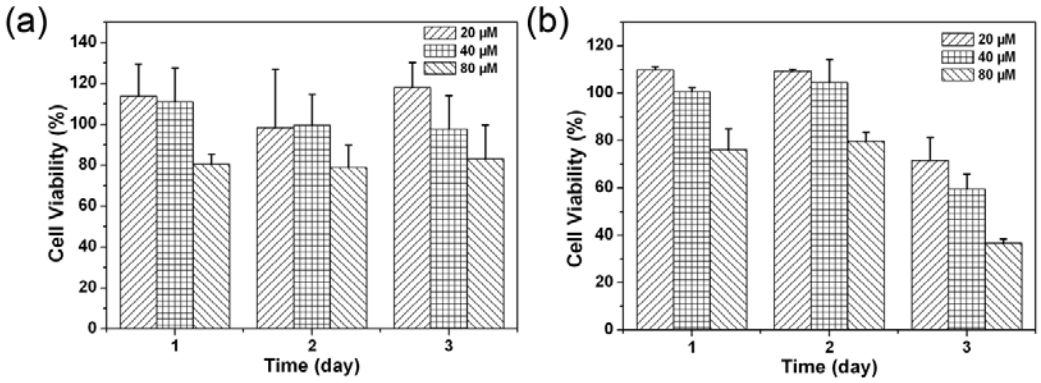

Figure S12. MTT assay of **1** on (a) HepG2 cells, and (b) LoVo cells. Cell viability values (%) estimated by MTT proliferation test at concentrations of 20, 40 and 80 μM of **1**. HepG2 cells, or LoVo cells were cultured in the presence of **1** for 1, 2 and 3 day at 37 °C under 5% CO_2. These experiments were performed in triplicate. Results are representative of three independent experiments. Error bars represent standard deviations.

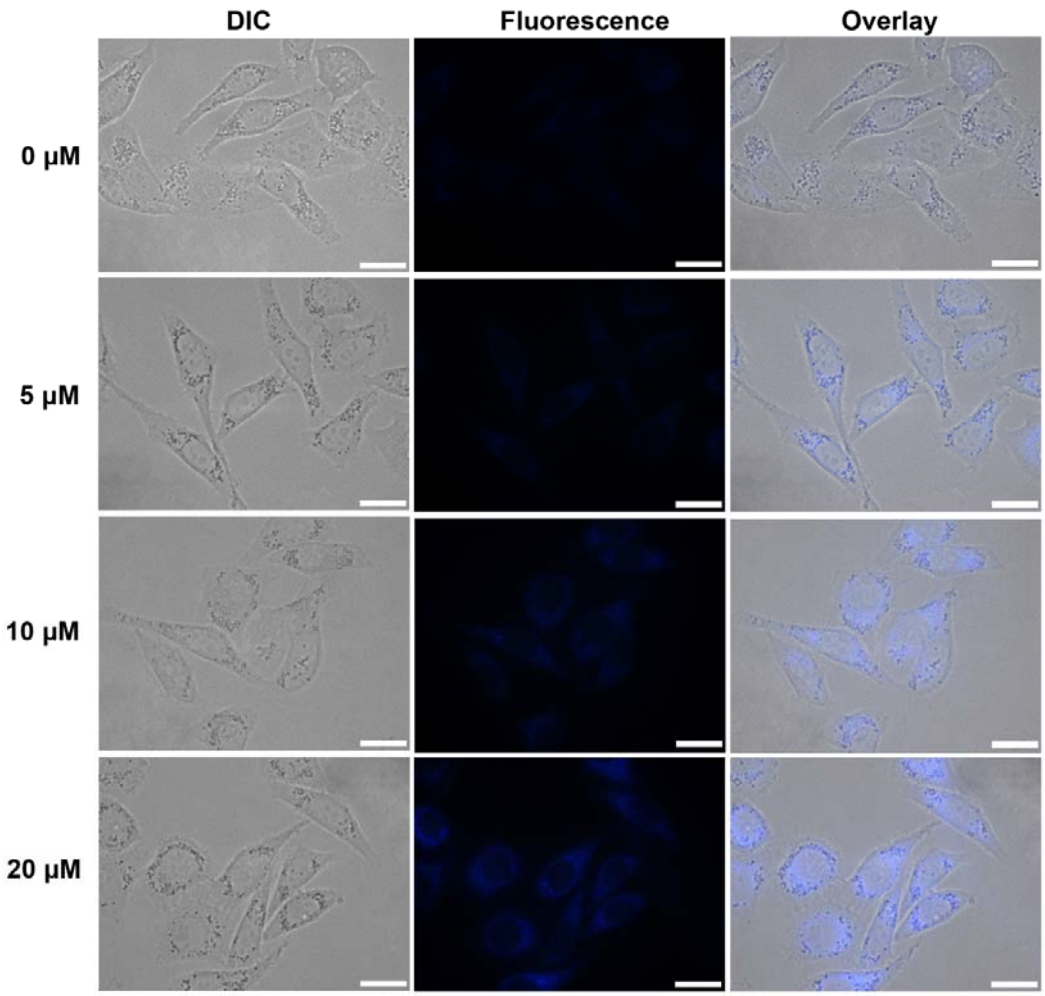

Figure S13. Differential interference contrast (DIC) images (left), fluorescence images (middle, DAPI channel), and merged images (right) of LoVo cells incubated with 0, 5, 10, or 20 μM of Cd^{2+} in serum-free medium for 30 min at 37 °C, washed with PBS for three times, then incubated with 20 μM **1** in serum-free medium for 0.5 h at 37 °C prior to imaging, respectively. Scale bar: 20 μm.

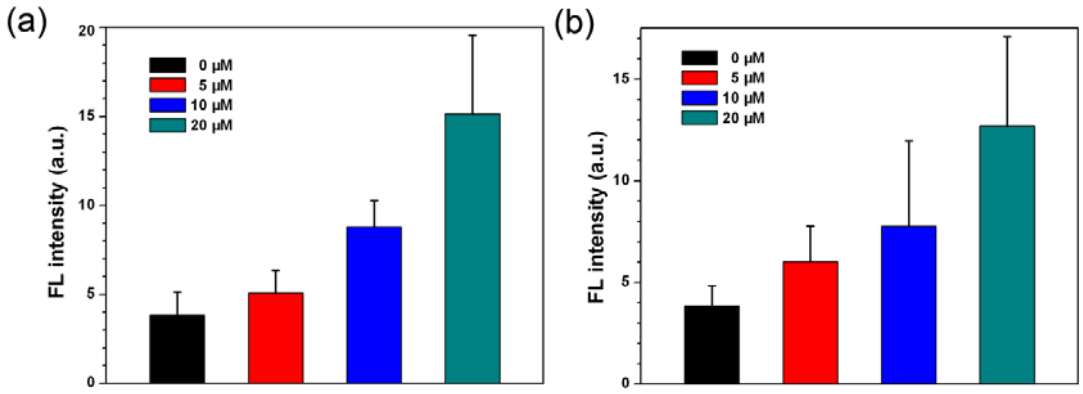

Figure S14. (a) The average fluorescence intensity of HepG2 cells in Figure 4. (b) The average fluorescence intensity of LoVo cells in Figure S13.

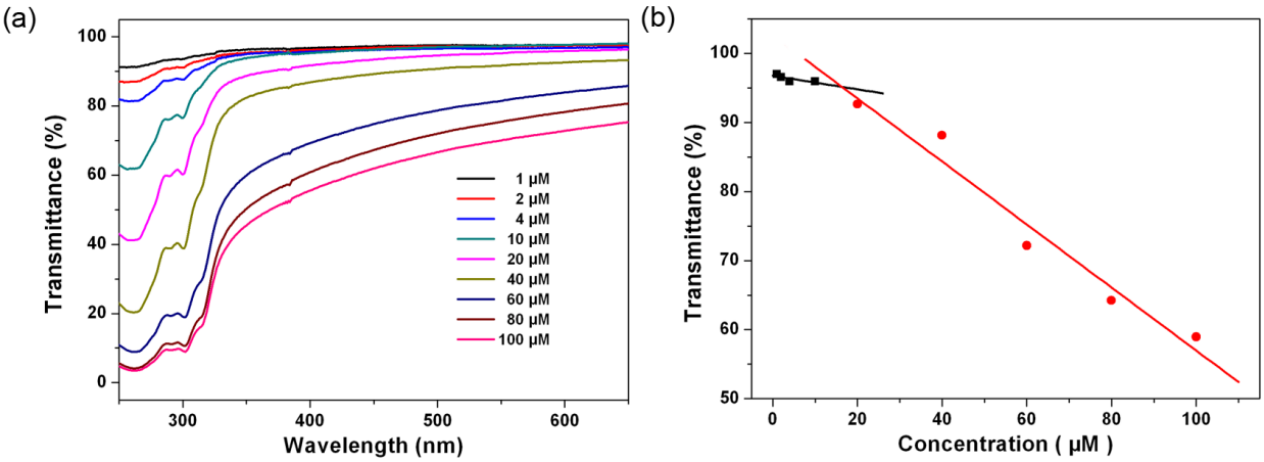

Figure S15. (a) UV−vis transmittance spectra of **1** at various concentrations in water (pH 5.5). (b) Concentration-dependent optical transmittance of **1** at 425 nm in water (pH 5.5).

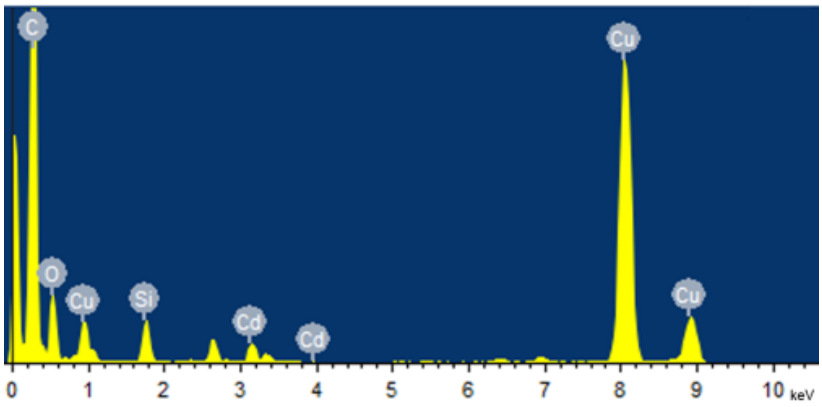

Figure S16. Energy-dispersive X-ray spectroscopic (EDS) elemental analysis of nanofibers in Figure 6c.

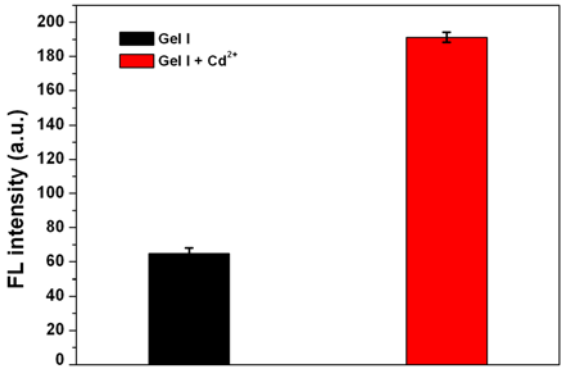

Figure S17. The average fluorescence intensity in Figures 6b & d.

3. Supporting Tables.

Table S1. HPLC condition for the purification of **1**.

Time (minute)	Flow (mL/min.)	H_2O %	CH_3CN%
0	3.0	30	70
3	3.0	30	70
35	3.0	0	100
37	3.0	0	100
38	3.0	30	70
40	3.0	30	70

Table S2. Using **1** to detect of Cd^{2+} in pond water (from east campus of USTC).

Sample	Level added (μM)	Level found (μM)	Recovery (%)	SD (μM)	RSD (%)
pond water	10	9.71	97	0.039	0.406
		9.66	96		
		9.64	96		

Table S3. Statistics of sensitivity of **1** and other reported methods for the detection of Cd^{2+}.

Method \ **LOD**		**The limit of detection (LOD) of Cd^{2+}**
Fluorometry	In this paper	2.10×10^{-8} M
	Cheng *et al.* reported a small molecule-based chemosensors[1]	1.00×10^{-7} M
	Varriale *et al.* reported protein-based sensing systems[2]	5.00×10^{-7} M
Atomic absorption spectrometry (AAS)[3]		4.20×10^{-11} M
Inductively coupled plasmas-Atomic fluorescence spectrometry (ICP-AFS)[4]		3.56×10^{-9} M
Inductively coupled plasmas-atomic emission spectrometry(ICP-AES)[5]		1.78×10^{-6} M
Inductively coupled plasma mass spectrometry (ICP-MS)[6]		8.90×10^{-11} M
X-ray fluorescence[7]		1.78×10^{-4} - 1.27×10^{-3} M
Liquid chromatography with electrochemical or spectrophotometric detection[8]		8.90×10^{-7} M for electrochemical detection; 1.78×10^{-8} M for spectrophotometric detection
Surface enhanced Raman scattering (SERS)[9]		1.00×10^{-6} M

4. References.

1 T. Y. Cheng, Y. F. Xu, S. Y. Zhang, W. P. Zhu, X. H. Qian and L. P. Duan, *J. Am. Chem. Soc.*, 2008, **130**, 16160-16161.

2 A. Varriale, M. Staiano, M. Rossi and S. D'Auria, *Anal. Chem.*, 2007, **79**, 5760-5762.

3 D. Colbert, K. S. Johnson and K. H. Coale, *Anal. Chim. Acta* 1998, **377**, 255-262.
4 A. Montaser and V. A. Fassel, *Anal. Chem.*, 1976, **48**, 1490-1499.
5 A. C. Davis, C. P. Calloway and B. T. Jones, *Talanta*, 2007, **71**, 1144-1149.
6 S. N. Willie, Y. Iida and J. W. McLaren, *Atom. Spectrosc.*, 1998, **19**, 67-72.
7 L. Ahlgren and S. Mattsson, *Phys. Med. Biol.*, 1981, **26**, 19-26.
8 A. M. Bond and G. G. Wallace, *Anal. Chem.*, 1984, **56**, 2085-2090.
9 J. Yin, T. Wu, J. B. Song, Q. Zhang, S. Y. Liu, R. Xu and H. W. Duan, *Chem. Mater.*, 2011, **23**, 4756-4764.